Math. Model. Nat. Phenom.
Vol. 12, No. 1, 2017, pp. 1–14
DOI: 10.1051/mmnp/201712101

Approximate Conservation Laws for an Integrable Boussinesq System

A. Ali[1], B.-S. Juliussen[2], H. Kalisch[2] *

[1] Nansen Environmental and Remote Sensing Center, 5006 Bergen, Norway

[2] Department of Mathematics, University of Bergen, Postbox 7800, 5020 Bergen, Norway

Abstract. The so-called Kaup-Boussinesq system is a model for long waves propagating at the surface of a perfect fluid. In this work, a derivation of approximate local conservation equations associated to the Kaup-Boussinesq system is given. The derivation of the approximate balance laws is based on reconstruction of the velocity field and the pressure in the fluid column below the free surface, and yields expressions for mass, momentum and energy densities and the corresponding fluxes. It is shown that the total energy found with this method is equal to the Hamiltonian functional featuring in the work of Craig and Groves [10].

For the numerical approximation of solutions to the Kaup-Boussinesq system, a filtered spectral method is put forward and shown to be stable when coupled with a convergent time-stepping scheme. The spectral method is used to confirm the exact conservation of the total momentum and energy.

Keywords and phrases: Mechanical balance laws, Long wave equations, Water waves, Hamiltonian models

Mathematics Subject Classification: 35Q35, 35Q51, 35Q53, 37Q10, 76B15

1. Introduction

The purpose of this work is the derivation of expressions for the mass, momentum and energy densities and the corresponding fluxes associated to an integrable system of evolution equations modeling the propagation of weakly nonlinear long waves on the surface of an incompressible, inviscid fluid. The equation under study is the so-called Kaup-Boussinesq system

$$\begin{aligned} &\eta_t + h_0 w_x + (\eta w)_x + \frac{h_0^3}{3} w_{xxx} = 0, \\ &w_t + g\eta_x + w w_x = 0, \end{aligned} \tag{1.1}$$

where $\eta(x,t)$ describes the deflection of the free surface from the rest position at a point x and time t, $w(x,t)$ is the horizontal velocity of the fluid at the free surface, g represents the gravitational acceleration, and h_0 denotes the undisturbed depth of the fluid.

The Kaup-Boussinesq system belongs to a family of long-wave models developed by Boussinesq [8], extended by Peregrine [25] and Nwogu [24] and many others, and represents a special case of the general

*Corresponding author. E-mail: henrik.kalisch@uib.no

system of long-wave models derived in [5]. These models describe the propagation of surface gravity waves of small amplitude and long wavelength in a horizontal channel of uniform depth, and under the assumption that the flow is irrotational and two-dimensional.

The derivation of such Boussinesq models for surface water waves is based on the assumption that there is an approximate balance between nonlinear steepening effects and dispersive spreading [5, 31]. Supposing that a is a representative amplitude, and ℓ represents a dominant wavelength, the Boussinesq scaling regime describes waves for which the two small parameters $\alpha = a/h_0 \ll 1$ and $\beta = h_0^2/\ell^2 \ll 1$ are approximately equal.

Even though the system (1.1) is not linearly well posed in the Hadamard sense [6], it is important because it has an integrable Hamiltonian structure [18] and exact solitary-wave solutions. Moreover, (1.1) appears naturally when the derivation of the long-wave system is based on approximating the Hamiltonian function of the full surface water-wave problem. As explained in detail in [10], this formulation is given in terms of the evaluation of the velocity potential at the free surface, and relies on the Hamiltonian structure of the full water wave problem found by Zakharov [32]. A version of this system also appears in the context of interfacial waves if it is required that an approximate Hamiltonian function be conserved [12].

The surface water-wave problem is generally described by the Euler equations with a slip boundary condition at the bottom, and kinematic and dynamic boundary conditions at the free surface. Assuming weak transverse effects, the unknowns are the surface elevation $\eta(x,t)$, the horizontal and vertical fluid velocities $u_1(x,z,t)$ and $u_2(x,z,t)$, respectively, and the pressure $P(x,z,t)$. If the assumption of irrotational flow is made, then a velocity potential $\phi(x,z,t)$ can be used. The problem may be posed on a domain $\{(x,z) \in \mathbb{R}^2 | -h_0 < z < \eta(x,t)\}$ which extends to infinity in the positive and negative x-direction. Due to the incompressibility of the fluid, the potential then satisfies Laplace's equation in this domain. The fact that the fluid cannot penetrate the bottom is expressed by a homogeneous Neumann boundary condition at the flat bottom. Thus we have the problem

$$\begin{aligned} \phi_{xx} + \phi_{zz} = 0 \text{ in } -h_0 < z < \eta(x,t) \\ \phi_z = 0 \text{ on } z = -h_0. \end{aligned}$$

We assume that the density is unity, and eliminate the pressure with help of the Bernoulli equation. The free-surface boundary conditions are then formulated in terms of the potential and the surface excursion by

$$\left.\begin{aligned} \eta_t + \phi_x\eta_x - \phi_z = 0, \\ \phi_t + \tfrac{1}{2}\left(\phi_x^2 + \phi_z^2\right) + g\eta = 0, \end{aligned}\right\} \text{ on } z = \eta(x,t).$$

The total energy of the system is given by the sum of potential and kinetic energy, and is normalized such that the potential energy is zero when no wave motion is present at the surface. Accordingly the Hamiltonian function for this problem is

$$H = V + K = \int_{\mathbb{R}} \int_0^{\eta} z \, dzdx + \int_{\mathbb{R}} \int_{-h_0}^{\eta} \frac{1}{2} |\nabla\phi|^2 \, dzdx.$$

Defining the trace of the potential at the free surface as $\Phi(x,t) = \phi(x,\eta(x,t),t)$, one may integrate in z in the first integral and use the divergence theorem on the second integral in order to arrive at the formulation

$$H = \frac{1}{2} \int_{\mathbb{R}} \left\{\eta^2 + \Phi G(\eta)\Phi\right\} \, dx.$$

This is the Hamiltonian formulation of the water wave problem as found in [13, 26, 32], and written in terms of the Dirichlet-Neumann operator $G(\eta)$. As shown in [23], the Dirichlet-Neumann operator is analytic in a certain sense and can be expanded as a power series as

$$G(\eta)\Phi = \sum_{j=0}^{\infty} G_j(\eta)\Phi. \tag{1.2}$$

The water-wave problem can be written in terms of G in the following form:

$$\begin{aligned}&\eta_t - G(\eta)\Phi = 0,\\ &\Phi_t + g\eta + \tfrac{1}{2}\Phi_x^2 - \tfrac{[G(\eta)\Phi+\eta_x\Phi_x]^2}{2(1+\eta_x^2)} = 0.\end{aligned}$$

Using the expansion (1.2), and the Boussinesq scaling mentioned above, it is straightforward to give a formal derivation of (1.1). This procedure can be made mathematically rigorous by introducing a symmetrized system as an intermediate step [7].

A different formal derivation of (1.1) is based on approximating the Hamiltonian. Such an approach was used in [10], and it was found that the approximate Hamiltonian is

$$H = \int_{-\infty}^{\infty} \left\{ \tfrac{g}{2}\eta^2 + \tfrac{1}{2}(h_0+\eta)w^2 - \tfrac{h_0^3}{6}w_x^2 \right\} dx. \tag{1.3}$$

Using this Hamiltonian, the system (1.1) appears naturally as the associated Hamiltonian dynamical system, and as shown in [18], the system (1.1) is actually a completely integrable system.

Since the derivation of (1.1) presented in [10] is based on approximating the total energy of the fluid system governed by the Euler equations, the integral (1.3) appears naturally as the total energy of the system in the approximation leading to (1.1). On the other hand, for some purposes it can also be of value to have knowledge of the energy contained in a smaller section of the fluid, and in particular of the local energy flux. These quantities can be important in various situations of practical significance, such as the modeling of undular bores [1, 31], tsunamis [14] and run-up of waves on beaches [17, 19, 29, 30].

The method of derivation used in [10], and related work such as [11, 22] has not been used to find expressions for energy flux, and it is not clear how to proceed in this context. However, in [2,3], a method was developed to derive mass, momentum and energy densities and fluxes associated to the family of Boussinesq systems found in [5]. We use the method of [2, 3], but with a different definition for the potential energy in order to show that the Hamiltonian function (1.3) represents the total energy in the system. Since the procedure is similar for mass density and flux, and for momentum density and flow force these quantities are also found.

A synopsis of the procedure can be stated as follows. The system (1.1) is obtained by neglecting terms of order $\alpha\beta$ and β^2 in the governing Euler equations. In order to obtain a corresponding approximation for the energy flux E and energy density q_E, one may stipulate that the differential energy balance equation

$$\frac{\partial}{\partial t}E + \frac{\partial}{\partial x}q_E = 0$$

hold to the same order in α and β as the evolution equations. Similar considerations yield expressions for the mass and momentum densities and the corresponding fluxes.

The plan of the paper is as follows. In section 2, the derivation of the Kaup-Boussinesq system is reviewed. In section 3, expressions for mass, momentum and energy densities and fluxes are found. These expressions are given in terms of the dependent variables η and w of the Kaup-Boussinesq system. Finally, in section 4, a spectral projection of (1.1) is put forward, and it is shown that the system conserves total momentum and energy.

2. Preliminaries

To set the stage for approximating the energy density and flux, we briefly recall the derivation of the Kaup-Boussinesq system using the method explained in [31]. In order to identify the relevant terms in the equations, the variables are non-dimensionalized as follows:

$$\tilde{x} = \frac{x}{\ell}, \quad \tilde{z} = \frac{z+h_0}{h_0}, \quad \tilde{\eta} = \frac{\eta}{a}, \quad \tilde{t} = \frac{c_0 t}{\ell}, \quad \tilde{\phi} = \frac{c_0}{ga\ell}\phi.$$

Here the limiting long-wave speed is given by $c_0 = \sqrt{gh_0}$. The free-surface boundary conditions then take the form

$$\left.\begin{aligned} \tilde{\eta}_{\tilde{t}} + \alpha\tilde{\phi}_{\tilde{x}}\tilde{\eta}_{\tilde{x}} - \tfrac{1}{\beta}\tilde{\phi}_{\tilde{z}} = 0, \\ \tilde{\eta} + \tilde{\phi}_{\tilde{t}} + \tfrac{1}{2}\big(\alpha\tilde{\phi}_{\tilde{x}}^2 + \tfrac{\alpha}{\beta}\tilde{\phi}_{\tilde{z}}^2\big) = 0, \end{aligned}\right\} \text{ on } \tilde{z} = 1 + \alpha\tilde{\eta}. \tag{2.1}$$

One may develop the potential ϕ in a formal asymptotic series and use the Laplace equation with Neumann boundary condition at the bed to express the non-dimensional velocity potential $\tilde{\phi}$ as

$$\tilde{\phi} = \tilde{f} - \frac{\tilde{z}^2}{2}\tilde{f}_{\tilde{x}\tilde{x}}\beta + \frac{\tilde{z}^4}{24}\tilde{f}_{\tilde{x}\tilde{x}\tilde{x}\tilde{x}}\beta^2 + \mathcal{O}(\beta^2). \tag{2.2}$$

Substituting this expression into the dynamic condition at the free surface leads to

$$\tilde{\eta} + \tilde{f}_{\tilde{t}} - \frac{\beta}{2}\tilde{f}_{\tilde{x}\tilde{x}\tilde{t}} + \frac{\alpha}{2}\tilde{f}_{\tilde{x}}^2 = \mathcal{O}(\alpha\beta, \beta^2). \tag{2.3}$$

To find a closed system of two evolution equations, we substitute the expression for $\tilde{\phi}$ in the kinematic boundary condition (2.1). Collecting terms of up to first order in α and β, differentiating (2.3), and expressing the equations in terms of the non-dimensional horizontal velocity at the bottom $f_{\tilde{x}} = \tilde{v}$ yields the equations

$$\begin{aligned} &\tilde{\eta}_{\tilde{t}} + \tilde{v}_{\tilde{x}} + \alpha(\tilde{\eta}\tilde{v})_{\tilde{x}} - \frac{1}{6}\beta\tilde{v}_{\tilde{x}\tilde{x}\tilde{x}} = \mathcal{O}(\alpha\beta, \beta^2), \\ &\tilde{\eta}_{\tilde{x}} + \tilde{v}_{\tilde{t}} - \frac{1}{2}\beta\tilde{v}_{\tilde{x}\tilde{x}\tilde{t}} + \alpha\tilde{v}\tilde{v}_{\tilde{x}} = \mathcal{O}(\alpha\beta, \beta^2). \end{aligned} \tag{2.4}$$

Now if $\tilde{w}$ denotes the nondimensional velocity at a nondimensional height $\tilde{z} = 1$ in the fluid column, then $\tilde{v}$ may be expressed in terms of $\tilde{w}$ as

$$\tilde{v} = \tilde{w} + \frac{1}{2}\beta\tilde{w}_{\tilde{x}\tilde{x}} + \mathcal{O}(\beta^2). \tag{2.5}$$

Writing (2.4) in terms of w, the system appears in the non-dimensional form

$$\begin{aligned} &\tilde{\eta}_{\tilde{t}} + \tilde{w}_{\tilde{x}} + \alpha(\tilde{\eta}\tilde{w})_{\tilde{x}} + \frac{1}{3}\beta\tilde{w}_{\tilde{x}\tilde{x}\tilde{x}} = \mathcal{O}(\alpha\beta, \beta^2), \\ &\tilde{\eta}_{\tilde{x}} + \tilde{w}_{\tilde{t}} + \alpha\tilde{w}\tilde{w}_{\tilde{x}} = \mathcal{O}(\alpha\beta, \beta^2). \end{aligned}$$

If terms of order $\mathcal{O}(\alpha\beta, \beta^2)$ are disregarded, and dimensional variables are used, the Kaup-Boussinesq system (1.1) is obtained.

As the aim here is to find expressions for the energy density and flux, it is essential to derive an approximation for the pressure associated to the (1.1), and we follow the method laid down in [2]. With the help of the Bernoulli equation, the dynamic pressure can be written as

$$P' = P + gz = -\phi_t - \frac{1}{2}|\nabla\phi|^2,$$

where atmospheric pressure has been set as the reference pressure, and the assumption that the density is equal to one has been used. Converting to non-dimensional variables, using the asymptotic expansion for the velocity potential (2.2), and using the identity (2.3), the second-order dynamic pressure emerges in the form

$$\tilde{P}' = \tilde{\eta} + \frac{1}{2}\beta(\tilde{z}^2 - 1)\tilde{w}_{\tilde{x}\tilde{t}} + \mathcal{O}(\alpha\beta, \beta^2).$$

Converting to dimensional variables, it might be confirmed that this agrees with the expression for the pressure associated to the so-called 'classical' Boussinesq system given in [27].

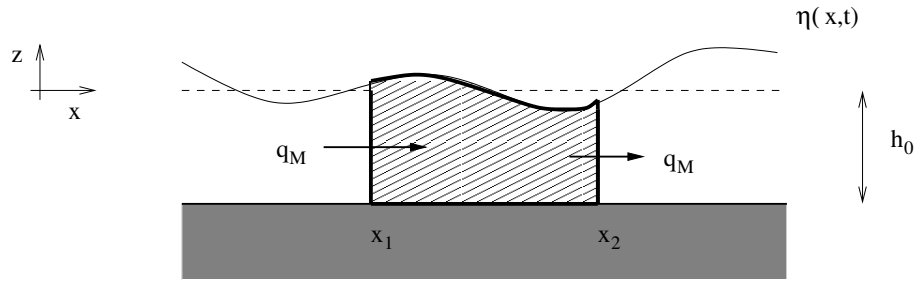

FIGURE 1. The schematic elucidates the geometric setup of the problem. The undisturbed water depth is h_0, and the x-axis is aligned with the free surface at rest. The free surface is described by a function $\eta(x,t)$. The figure shows a control interval delimited by x_1 and x_2 on the abscissa, and the arrows indicate the mass flux q_M.

3. Approximate balance laws

As solutions of the Kaup-Boussinesq system (1.1) are approximations of the more fundamental flow variables governed by the full water-wave problem laid down in the Introduction, it appears that conservation of mass, momentum and energy may only hold approximately. The purpose of this section is the derivation of approximate densities and fluxes which are connected to the Kaup-Boussinesq system.

3.1. Mass

For the conservation of mass, we consider the balance in a control volume in the fluid, such as depicted in Figure 1. Note that we are working with a two-dimensional approximation, so that all quantities have to be interpreted as being per unit span in the transverse direction. Recall also that the density is assumed to be unity. The change in mass in the control volume delimited by x_1 and x_2 in the x-direction is given by the flux through the lateral boundaries so that we have

$$\frac{d}{dt}\int_{x_1}^{x_2}\int_{-h_0}^{\eta} dzdx = \left[\int_{-h_0}^{\eta} \phi_x \, dz\right]_{x_2}^{x_1}.$$

Now we transform to non-dimensional variables, integrate with respect to $\tilde{z}$, write out the expression for $\tilde{\phi}_x$ and use the relation (2.5) to obtain

$$\frac{d}{d\tilde{t}}\int_{x_1/l}^{x_2/l}(1+\alpha\tilde{\eta})d\tilde{x} = \alpha\left[\tilde{w}+\alpha\tilde{w}\tilde{\eta}+\frac{\beta}{3}\tilde{w}_{\tilde{x}\tilde{x}}+O(\alpha\beta,\alpha^2)\right]_{x_2/l}^{x_1/l}.$$

Further, we divide by the length of the interval, and take the limit $x_2/l \to x_1/l$. Then the differential balance equation for mass is obtained as

$$\tilde{\eta}_{\tilde{t}}+\tilde{w}_{\tilde{x}}+\alpha(\tilde{w}\tilde{\eta})_{\tilde{x}}+\frac{\beta}{3}\tilde{w}_{\tilde{x}\tilde{x}\tilde{x}} = O(\alpha\beta,\beta^2).$$

This can be written as

$$\frac{\partial}{\partial\tilde{t}}\tilde{M}+\frac{\partial}{\partial\tilde{x}}\tilde{q}_M = O(\alpha^2\beta,\alpha\beta^2), \tag{3.1}$$

when the non-dimensional mass and density are given by

$$\tilde{M} = 1+\alpha\tilde{\eta},$$
$$\tilde{q}_M = \alpha\tilde{w}+\alpha^2\tilde{\eta}\tilde{w}+\frac{1}{3}\alpha\beta\tilde{w}_{\tilde{x}\tilde{x}}.$$

In dimensional variables, we have

$$M = h_0 + \eta,$$
$$q_M = h_0 w + \rho\eta w + \frac{1}{3}h_0^3 w_{xx},$$

where the scalings $M = h_0\tilde{M}$ and $q_M = h_0 c_0 \tilde{q}_M$ are used. It now appears that the first equation of (1.1) can be written as $\frac{\partial}{\partial t}M + \frac{\partial}{\partial x}q_M = 0$, so that mass is exactly conserved in the approximation described by the Kaup-Boussinesq system.

3.2. Momentum

For the case of momentum conservation, the change in momentum in the control volume is equal to the sum of the momentum flux through the boundaries and the net pressure force. In terms of the variables appearing in the full water-wave problem, this balance is described by

$$\frac{d}{dt}\int_{x_1}^{x_2}\int_{-h_0}^{\eta}\phi_x\, dzdx = \left[\int_{-h_0}^{\eta}\phi_x^2\, dz + \int_{-h_0}^{\eta} P\, dz\right]_{x_2}^{x_1}.$$

Transforming to non-dimensional variables, substituting the expressions for $\tilde{\phi}_x$ and the total pressure based on the dynamic pressure found in the introduction (cf. [2]), and again using the relation (2.5), the following differential balance equation is obtained:

$$\tilde{w}_{\tilde{t}} + \alpha(\tilde{w}\tilde{\eta})_{\tilde{t}} + \frac{\beta}{3}\tilde{w}_{\tilde{x}\tilde{x}\tilde{t}} + \tilde{\eta}_{\tilde{x}} + 2\alpha\tilde{w}\tilde{w}_{\tilde{x}} + \alpha\tilde{\eta}\tilde{\eta}_{\tilde{x}} - \frac{1}{3}\beta\tilde{w}_{\tilde{x}\tilde{x}\tilde{t}} = O(\alpha^2, \alpha\beta, \beta^2). \tag{3.2}$$

Setting

$$\tilde{I} = \alpha\tilde{w} + \alpha^2\tilde{w}\tilde{\eta} + \frac{1}{3}\alpha\beta\tilde{w}_{\tilde{x}\tilde{x}},$$
$$\tilde{q}_I = \alpha\tilde{\eta} + \alpha^2\tilde{w}^2 + \frac{1}{2}\alpha^2\tilde{\eta}^2 - \frac{1}{3}\alpha\beta\tilde{w}_{\tilde{x}\tilde{t}} + \frac{1}{2}, \tag{3.3}$$

the momentum balance can be written as

$$\frac{\partial}{\partial\tilde{t}}\tilde{I} + \frac{\partial}{\partial\tilde{x}}\tilde{q}_I = O(\alpha^3, \alpha^2\beta, \alpha\beta^2). \tag{3.4}$$

In dimensional form, with scalings $I = h_0 c_0 \tilde{I}$ and $q_I = h_0 c_0^2 \tilde{q}_I$, we get

$$I = (h_0 + \eta)w + \frac{1}{3}h_0^3 w_{xx},$$
$$q_I = h_0 w^2 + \frac{1}{2}g(h_0 + \eta)^2 - \frac{1}{3}h_0^3 w_{xt}$$

Note that the term q_I incorporates both the momentum flux and the pressure force. Especially in the context of steady flows, this term is sometimes called flow force [4]. While local momentum conservation holds only approximately, it can be shown that I and q_I satisfy the relation $\frac{\partial}{\partial t}I + \frac{\partial}{\partial x}q_I = \frac{\partial}{\partial x}\mathcal{F}$, for a certain function $\mathcal{F}$. With this, it is clear that conservation of total momentum holds in the Kaup-Boussinesq model.

3.3. Energy

In order to find expressions for the energy density and flux we consider the mechanical energy inside a control volume in the fluid and above the interval $[x_1, x_2]$, as shown in Figure 1. The mechanical energy in this control volume is

$$\mathcal{E} = \frac{1}{2}\int_{x_1}^{x_2}\int_{-h_0}^{\eta}|\nabla\phi|^2 dzdx + \int_{x_1}^{x_2}\int_{0}^{\eta} gz\, dzdx,$$

where the first term represents the kinetic energy. The second term is the potential energy which has been normalized in such a way that the total potential energy is zero when no wave motion is present. Following [28], conservation of mechanical energy is written as

$$\frac{d}{dt}\int_{x_1}^{x_2}\int_{-h_0}^{\eta}\frac{1}{2}|\nabla\phi|^2\,dzdx+\frac{d}{dt}\int_{x_1}^{x_2}\int_{0}^{\eta}gz\,dzdx=\left[\int_{-h_0}^{\eta}\left\{\tfrac{1}{2}|\nabla\phi|^2+gz\right\}\phi_x\,dz+\int_{-h_0}^{\eta}\phi_x P\,dz\right]_{x_2}^{x_1}.$$

We convert to non-dimensional variables and substitute the expressions for $\tilde{\phi}_{\tilde{x}}$ and $\tilde{\phi}_{\tilde{z}}$, recalling that $f_{\tilde{x}}=\tilde{v}$ is the velocity at the bottom, and using (2.5). Thus the energy balance equation transforms to

$$\begin{aligned}\frac{d}{d\tilde{t}}\int_{x_1/\ell}^{x_2/\ell}\left\{\frac{\alpha^2}{2}\tilde{\eta}^2+\frac{\alpha^2}{2}(1+\alpha\tilde{\eta})\tilde{w}^2+\frac{\alpha^2\beta}{3}\tilde{w}\tilde{w}_{\tilde{x}\tilde{x}}+\frac{\alpha^2\beta}{6}\tilde{w}_{\tilde{x}}^2\right\}\,d\tilde{x}\\ =\left[\frac{\alpha^3}{2}\tilde{w}^3+\alpha^2\tilde{w}\tilde{\eta}(1+\alpha\tilde{\eta})+\frac{\alpha^2\beta}{3}\tilde{\eta}\tilde{w}_{\tilde{x}\tilde{x}}-\frac{\alpha^2\beta}{3}\tilde{w}\tilde{w}_{\tilde{x}\tilde{t}}\right]_{x_2}^{x_1}+\mathcal{O}(\alpha^4,\alpha^3\beta,\alpha^2\beta^2).\end{aligned}\tag{3.5}$$

A differentiation in x finally yields the differential energy balance equation in the form

$$\frac{\partial}{\partial\tilde{t}}\tilde{E}+\frac{\partial}{\partial\tilde{x}}\tilde{q}_E=\mathcal{O}(\alpha^2,\alpha\beta,\beta^2).\tag{3.6}$$

Taking the appropriate terms in the energy density and flux in (3.5) which are of order zero or one in the differential energy balance (3.6), we find the non-dimensional energy density per unit span to be

$$\tilde{E}=\frac{\alpha^2}{2}\tilde{\eta}^2+\frac{\alpha^2}{2}(1+\alpha\tilde{\eta})\tilde{w}^2+\frac{\alpha^2\beta}{3}\tilde{w}\tilde{w}_{\tilde{x}\tilde{x}}+\frac{\alpha^2\beta}{6}\tilde{w}_{\tilde{x}}^2.$$

The non-dimensional energy flux per unit span (including the work done by pressure force) is given by

$$\tilde{q}_E=\frac{\alpha^3}{2}\tilde{w}^3+\alpha^2\tilde{w}\tilde{\eta}(1+\alpha\tilde{\eta})+\frac{\alpha^2\beta}{3}\tilde{\eta}\tilde{w}_{\tilde{x}\tilde{x}}-\frac{\alpha^2\beta}{3}\tilde{w}\tilde{w}_{\tilde{x}\tilde{t}}.$$

Using the natural scalings $E=h_0c_0^2\tilde{E}$ and $q_E=h_0c_0^3\tilde{q}_E$, the dimensional forms of these quantities are obtained in the form

$$E=\left\{\frac{g}{2}\eta^2+\frac{1}{2}(h_0+\eta)w^2+\frac{h_0^3}{3}ww_{xx}+\frac{h_0^3}{6}w_x^2\right\},$$

and

$$q_E=\left\{\frac{h_0}{2}w^3+g\eta w(h_0+\eta)+\frac{gh_0^3}{3}\eta w_{xx}-\frac{h_0^3}{3}ww_{xt}\right\}.$$

In particular, $q_E(x,t)$ gives the energy flux plus the work done by the pressure force due to the wave motion at a point x and a time t. $E(x,t)$ is the approximate energy density, so that integrating $E(x,t)$ over an interval $[x_1,x_2]$ yields the energy due to the wave motion in the control interval shown in Figure 1 at a time t, and to the same order of approximation as the system (1.1) is valid. If the surface disturbance is localized, so that η and w decay to zero at infinity, and the integration of E is taken over the entire real line, an integration by parts shows that the total energy is equal to the Hamiltonian function derived by Craig and Groves [10]. In other words, we have $H=\int E\,dx$, where H is given by (1.3).

4. Spectral projection

We now turn to the numerical approximation of solutions to the Kaup-Boussinesq system (1.1). The method to be used here is a Fourier-collocation method coupled with a hybrid time-integration scheme which uses a Crank-Nicholson method for the linear part and an Adams-Bashforth method for the nonlinear terms. The reason for this choice is that the Crank-Nicolson method is neutrally stable for problems

with imaginary eigenvalues which is the case here. Moreover, there is no restriction on the time step, and the method can be evaluated explicitly if the problem is linear and diagonal. Using the same method for the nonlinear terms is possible, but now an iteration must be used. Since this diminishes the efficiency, we have opted instead for an explicit second-order Adams-Bashforth method. This method introduces some conditions on the time step, but usually the time step has to be chosen fairly small at any rate in order to achieve good accuracy.

For the efficient application of the Crank-Nicholson method, the linear part of the system is diagonalized. In order to explain the diagonalization, we first treat the linear part of the system separately.

4.1. The linearized system

The linearized system is written as

$$\begin{aligned} \eta_t &= -w_x - \tfrac{1}{3} w_{xxx}, \\ w_t &= -\eta_x. \end{aligned} \tag{4.1}$$

This system has an exact solution of the form

$$w(x,t) = \sin\left(\kappa x - \sqrt{1-\tfrac{\kappa^2}{3}}t\right),$$

$$\eta(x,t) = \sqrt{1-\tfrac{\kappa^2}{3}}\,\sin\left(\kappa x - \sqrt{1-\tfrac{\kappa^2}{3}}t\right),$$

which can be used to test the implementation of the numerical scheme. The system (4.1) can be written as

$$\begin{bmatrix} \eta_t \\ w_t \end{bmatrix} = \begin{pmatrix} 0 & -\frac{\partial}{\partial x} - \frac{1}{3}\frac{\partial^3}{\partial x^3} \\ -\frac{\partial}{\partial x} & 0 \end{pmatrix} \begin{bmatrix} \eta \\ w \end{bmatrix}.$$

When transformed into the Fourier space, the system takes the form

$$\begin{bmatrix} \hat{\eta}_t \\ \hat{w}_t \end{bmatrix} = ik \begin{pmatrix} 0 & \frac{k^2}{3} - 1 \\ -1 & 0 \end{pmatrix} \begin{bmatrix} \hat{\eta} \\ \hat{w} \end{bmatrix}. \tag{4.2}$$

To diagonalize, we find the eigenvalues of the matrix and the corresponding eigenvectors to be

$$\lambda_{1,2} = \pm\sqrt{1-\tfrac{k^2}{3}}, \quad \mathbf{a}_1 = \begin{bmatrix} \sqrt{1-\frac{k^2}{3}} \\ 1 \end{bmatrix}, \quad \mathbf{a}_2 = \begin{bmatrix} -\sqrt{1-\frac{k^2}{3}} \\ 1 \end{bmatrix}.$$

Now, using the relation

$$\begin{bmatrix} \hat{\eta} \\ \hat{w} \end{bmatrix} = \mathbf{T} \begin{bmatrix} \xi \\ \zeta \end{bmatrix},$$

where $\mathbf{T}$ is the matrix with the eigenvectors as columns

$$\mathbf{T} = \begin{bmatrix} \sqrt{1-\frac{k^2}{3}} & -\sqrt{1-\frac{k^2}{3}} \\ 1 & 1 \end{bmatrix},$$

we obtain the new diagonalized system in new variables ξ and ζ

$$\begin{bmatrix} \xi_t \\ \zeta_t \end{bmatrix} = ik \begin{pmatrix} \sqrt{1-\frac{k^2}{3}} & 0 \\ 0 & -\sqrt{1-\frac{k^2}{3}} \end{pmatrix} \begin{bmatrix} \xi \\ \zeta \end{bmatrix}. \tag{4.3}$$

Here, we have used that

$$\mathbf{D} = \mathbf{T}^{-1}\mathbf{A}\mathbf{T},$$

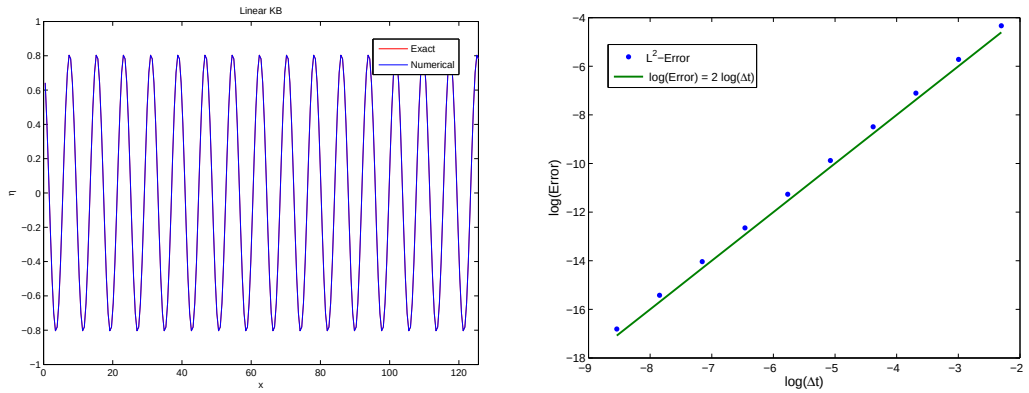

FIGURE 2. Left panel: Wave profile of the linear part of the Kaup-Boussinesq system for $\Delta t = 0.1$. No difference between the exact solutions and the numerical approximation can be discerned. Right panel: log – log scale plot of error against time step Δt. A line with slope 2 is added for convenience. Second-order convergence is apparent.

where $\mathbf{D}$ is the diagonal matrix in (4.3), and $\mathbf{A}$ is the original matrix in (4.2). $\mathbf{T}^{-1}$ is found to be

$$\mathbf{T^{-1}} = \begin{pmatrix} -\frac{1}{2\sqrt{1-k^2/3}} & \frac{1}{2} \\ \frac{1}{2\sqrt{1-k^2/3}} & \frac{1}{2} \end{pmatrix}.$$

Since the eigenvalues of the system are purely imaginary, a Crank-Nicolson method can be employed efficiently since it is stable for imaginary parts of the spectrum, and there is no condition on the size of the time step. Moreover, even though the method is implicit, it can be evaluated explicitly for diagonal system such as (4.3). For a time step Δt, the time stepping for the system (4.3) can be written as

$$\xi_{n+1} = \frac{1+\frac{1}{2}\Delta tik\sqrt{1-\frac{k^2}{3}}}{1-\frac{1}{2}\Delta tik\sqrt{1-\frac{k^2}{3}}}\xi_n, \qquad \zeta_{n+1} = \frac{1-\frac{1}{2}\Delta tik\sqrt{1-\frac{k^2}{3}}}{1+\frac{1}{2}\Delta tik\sqrt{1-\frac{k^2}{3}}}\zeta_n.$$

The initial conditions for η and w need to be transformed to the new variables using $\mathbf{T^{-1}}$. When the final time is reached, a transformation back to the original variables w and η is done using $\mathbf{T}$.

Now it is apparent from these formulas that it is not sufficient to rescale the problem in order to achieve numerical stability. For small values of the the spatial grid, i.e. large enough values of k, exponential growth cannot be avoided. Thus it is imperative to use a spectral filter, setting the amplitudes of all modes to zero unless

$$|k| < \sqrt{3}.$$

If we choose a filter so that this is satisfied, and with the same discretization as before, the method is very robust. We obtain the wave profile shown in Figure 2, and we observe second-order convergence in the size of the time step Δt (see right panel of Figure 2 and Table 1).

4.2. Numerical procedure for the full Kaup-Boussinesq system

Next, we investigate the full Kaup-Boussinesq system. Transforming the system to Fourier space, the following system is obtained:

$$\begin{bmatrix} \hat{\eta}_t \\ \hat{w}_t \end{bmatrix} = ik \begin{pmatrix} 0 & \frac{1}{3}k^2 - 1 \\ -1 & 0 \end{pmatrix} \begin{bmatrix} \hat{\eta} \\ \hat{w} \end{bmatrix} + \begin{bmatrix} -ik(\eta\hat{w}) \\ -ik\frac{1}{2}(\hat{w^2}) \end{bmatrix}.$$

	Results for η		Results for w	
Δt	L^∞**-error**	**ratio**	L^∞**-error**	**ratio**
0.1000	1.3933e-04		1.4852e-04	
0.0500	3.4844e-05	3.9986	3.7144e-05	3.9986
0.0250	8.7117e-06	3.9996	9.2867e-06	3.9996
0.0125	2.1780e-06	3.9999	2.3217e-06	3.9999
0.0063	5.4450e-07	4.0000	5.8044e-07	4.0000
0.0031	1.3612e-07	4.0000	1.4511e-07	4.0000
0.0016	3.4031e-08	4.0000	3.6277e-08	4.0000
7.8125e-04	8.5078e-09	4.0000	9.0693e-09	4.0000
3.9063e-04	2.1270e-09	4.0000	2.2673e-09	4.0000
1.9531e-04	5.3174e-10	4.0000	5.6684e-10	4.0000

TABLE 1. Errors and ratios for different time steps of the linear part of the Kaup-Boussinesq system.

In the same fashion as was done for the linear part, the system is diagonalized in order to uncouple the linear part. The eigenvalues of the matrix and the corresponding eigenvectors are the same, and we obtain the system

$$\begin{bmatrix}\xi_t\\ \zeta_t\end{bmatrix} = ik\begin{pmatrix}\sqrt{1-k^2/3} & 0\\ 0 & -\sqrt{1-k^2/3}\end{pmatrix}\begin{bmatrix}\xi\\ \zeta\end{bmatrix} + \mathbf{T^{-1}}\begin{bmatrix}-ik(\hat{\eta w})\\ -ik\frac{1}{2}(\hat{w^2})\end{bmatrix}. \tag{4.4}$$

Using again Crank-Nicolson on the linear terms and Adams-Bashforth on the nonlinear terms, we get the following algorithm:

$$\begin{aligned}
\xi_{n+1} &= \tfrac{1+\frac{1}{2}\Delta tik\sqrt{i-k^2/3}}{1-\frac{1}{2}\Delta tik\sqrt{i-k^2/3}}\xi_n + \tfrac{\frac{3}{4}\Delta t\frac{ik}{\sqrt{1-k^2/3}}}{1-\frac{1}{2}\Delta tik\sqrt{i-k^2/3}}\widehat{(\eta w)}_n + \tfrac{-\frac{3}{8}\Delta tik}{1-\frac{1}{2}\Delta tik\sqrt{i-k^2/3}}\widehat{(w^2)}_n +\\
&\tfrac{-\frac{1}{4}\Delta t\frac{ik}{\sqrt{1-k^2/3}}}{1-\frac{1}{2}\Delta tik\sqrt{i-k^2/3}}\widehat{(\eta w)}_{n-1} + \tfrac{\frac{1}{8}\Delta tik}{1-\frac{1}{2}\Delta tik\sqrt{i-k^2/3}}\widehat{(w^2)}_{n-1},\\
\zeta_{n+1} &= \tfrac{1-\frac{1}{2}\Delta tik\sqrt{i-k^2/3}}{1+\frac{1}{2}\Delta tik\sqrt{i-k^2/3}}\widehat{y}_n + \tfrac{-\frac{3}{4}\Delta t\frac{ik}{\sqrt{1-k^2/3}}}{1+\frac{1}{2}\Delta tik\sqrt{i-k^2/3}}\widehat{(\eta w)}_n + \tfrac{-\frac{3}{8}\Delta tik}{1+\frac{1}{2}\Delta tik\sqrt{i-k^2/3}}\widehat{(w^2)}_n +\\
&\tfrac{\frac{1}{4}\Delta t\frac{ik}{\sqrt{1-k^2/3}}}{1+\frac{1}{2}\Delta tik\sqrt{i-k^2/3}}\widehat{(\eta w)}_{n-1} + \tfrac{\frac{1}{8}\Delta tik}{1+\frac{1}{2}\Delta tik\sqrt{i-k^2/3}}\widehat{(w^2)}_{n-1}.
\end{aligned} \tag{4.5}$$

The numerical procedure is as follows:
- Transform the initial conditions from η and w to ξ and ζ, respectively.
- Filter the initial conditions
- Take the products ηw and w^2 in physical space, using DFT and inverse DFT
- Filter the products
- Iterate and filter the new ξ and ζ at each time step
- After the iterations, transform back to the original η and w in physical space.

4.3. Results

The code is tested using the exact solution

$$\begin{aligned}
w(x,t) &= \tfrac{2(c^2-1)}{\cosh(\sqrt{3(c^2-1)}(x-ct))+c},\\
\eta(x,t) &= cw(x,t) - \tfrac{1}{2}w^2(x,t).
\end{aligned} \tag{4.6}$$

The numerical results show that the method works quite well for small amplitude waves, confirming the basis for deriving the model in the first place. If the wave speed is chosen to be as small as $c = 1.005$ we get a good approximation with a small error, and we also get the correct order of convergence, as seen by the ratio 4 in Table 2. The wave profile is shown in Figure 3.

$c = 1.005$	Results for η		Results for w	
Δt	L^∞**-error**	**ratio**	L^∞**-error**	**ratio**
0.1000	2.5936e-08		2.0982e-08	
0.0500	6.4486e-09	4.0219	5.2118e-09	4.0258
0.0250	1.6077e-09	4.0111	1.2988e-09	4.0129
0.0125	4.0135e-10	4.0056	3.2417e-10	4.0064
0.0063	1.0027e-10	4.0029	8.0977e-11	4.0033
0.0031	2.5057e-11	4.0016	2.0235e-11	4.0019
0.0016	6.2619e-12	4.0014	5.0562e-12	4.0019
7.8125e-04	1.5638e-12	4.0042	1.2621e-12	4.0061
3.9063e-04	3.8951e-13	4.0149	3.1381e-13	4.0219
1.9531e-04	9.7469e-14	3.9963	8.0764e-14	3.8856

TABLE 2. Errors and ratio for different time steps of the Kaup-Boussinesq system. Results for η and w.

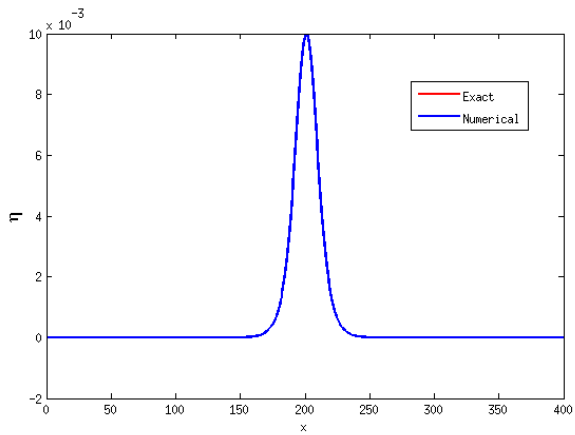

FIGURE 3. Wave profile for $c = 1.005$. The blue curve shows the computed solution at final time $T = 1$. The red curve shows the exact solution at evaluated at the same time.

For smaller wave speeds the waves get broader, so we have to increase the length of the interval L in order to get right order of convergence. For larger wave speeds, some instability is observed even though the computations can still be carried forward. Wave profiles of solitary waves with $c = 1.2$ and $c = 1.8$ are shown in Figure 4. It appears that larger-amplitude solitary waves are narrower, and contain too many high-frequency components, so that they cannot be adequately resolved with the filtered numerical scheme. For vary large amplitudes, the code becomes unstable, and the solution blows up after a few iterations.

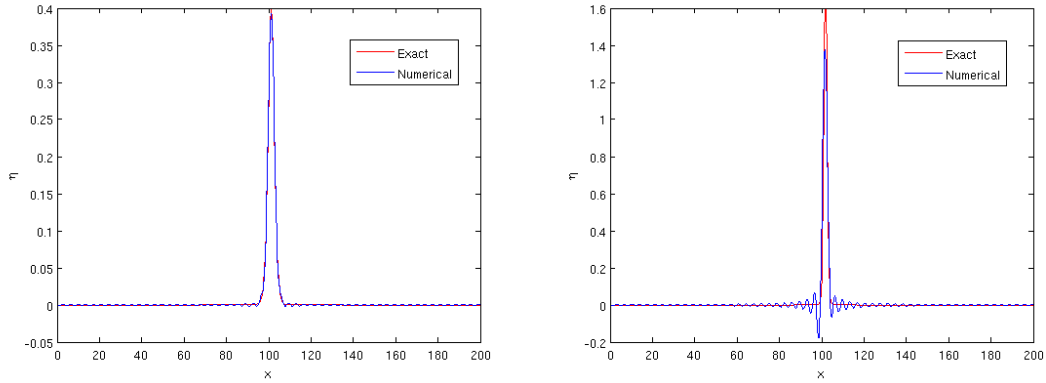

FIGURE 4. Waveprofiles for $c = 1.2$ and $c = 1.8$. The blue curves shows the computed solutions at final time $T = 1$. The red curves show the exact solution at evaluated at the same time.

4.4. Conservation of Momentum and Energy

For the interval $[0, L]$, we should have conservation mass, momentum and energy since periodicity is assumed. Conservation of mass is expressed by the first equation of (1.1), so we focus on momentum and energy. We use the differential conservation equations of the Kaup-Boussinesq system derived in Section 3 to see if conservation is satisfied with our method. Since these equations are given by w and η, we can use the quantities computed numerically. For the momentum differential balance equation, it was found that

$$\frac{\partial}{\partial t} I + \frac{\partial}{\partial x} q_I = \frac{\partial}{\partial x} \mathcal{F},$$

for a certain function $\mathcal{F}$, so that we have

$$\int_0^L I \, dx = \text{constant}.$$

Moreover, we also have

$$\frac{\partial}{\partial t} I = \frac{\partial}{\partial x} \mathcal{G},$$

for some function $\mathcal{G} \neq q_E$. Thus total energy is also conserved, i.e.

$$\int_0^L E \, dx = \text{constant}.$$

In the numerical code, these two integrals are evaluated at each time step, and it is found that they are conserved up to a very small error. Since the conservation is trivial for solitary waves, we test conservation with another initial condition where the numerical solution is clearly different from a simple translation, In Figure 5 the evolution for initial data

$$\eta(x, 0) = \frac{1.2}{\cosh\left(\sqrt{0.03x}\right) + 1}; \qquad w(x, 0) = \frac{1}{\cosh\left(\sqrt{0.03x}\right) + 1}; \tag{4.7}$$

is shown.

As can be seen from Figure 5, the numerical solution is clearly not translational, but conservation is still satisfied. For the plots of η and w, the final time is $T = 25$ with time step $\Delta t = 0.05$. The lower right

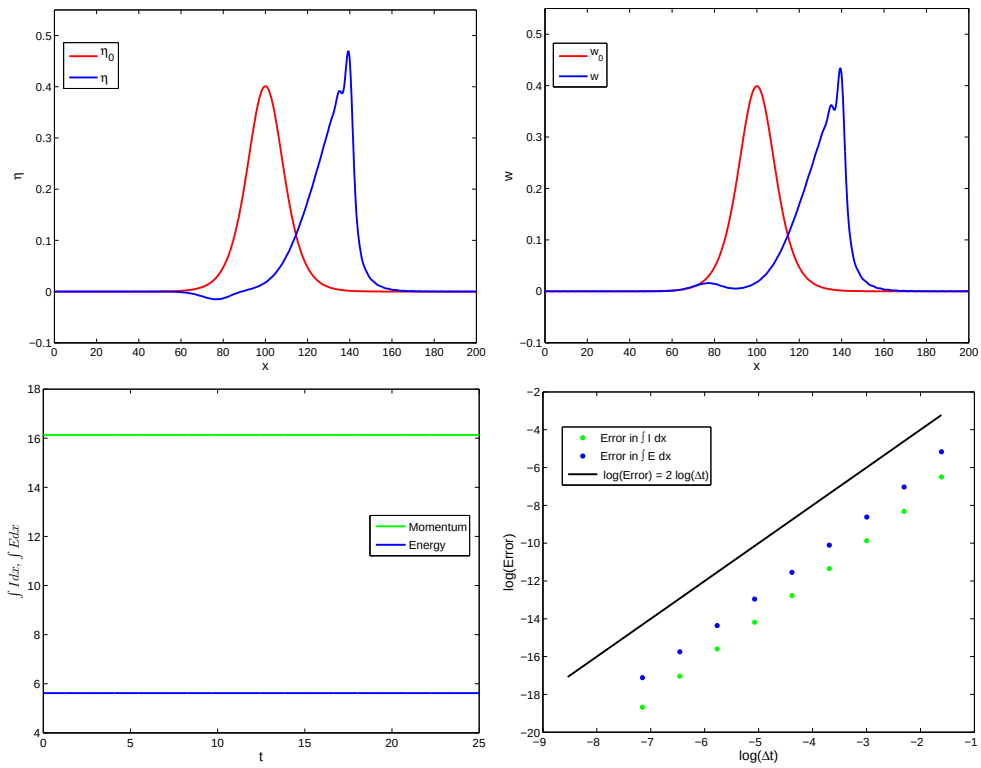

FIGURE 5. Upper panels: Initial condition and numerical solution for η and w. Lower left panel: The integrals of the momentum and energy plotted at each time step for initial data given by (4.7). Lower right panel: Order of convergence of the numerical method, as measured by the conserved integrals.

panel shows the convergence of the conserved quantities, where the error is defined by

$$\frac{|\int I(x,T)\ dx - \int I(x,0)\ dx|}{|\int I(x,0)\ dx|}$$

for the momentum, and accordingly for the energy. Indeed, 2-nd order convergence is clearly visible also in Table 3.

	Results for $\int I\ dx$		Results for $\int E\ dx$	
Δt	**Error**	**Ratio**	**Error**	**Ratio**
0.1000	2.58e-5		1.28e-4	
0.0500	5.92e-6	4.36	2.89e-5	4.43
0.0250	1.42e-6	4.16	6.88e-6	4.21
0.0125	3.50e-7	4.06	1.68e-6	4.10
0.0063	8.84e-8	3.97	4.14e-7	4.05
0.0031	2.36e-8	3.74	1.03e-7	4.03
0.0016	7.51e-9	3.14	2.56e-8	4.01

TABLE 3. Errors and ratio for different time steps of the Kaup-Boussinesq system. Results for $\int I\ dx$ and $\int E\ dx$.

Acknowledgements. This research was supported by the Research Council of Norway through grant no. NFR 213474/F20.

References

[1] A. Ali, H. Kalisch. *Energy balance for undular bores.* C. R. Mécanique 338 (2010), 67–70.
[2] A. Ali, H. Kalisch. *Mechanical balance laws for Boussinesq models of surface water waves.* J. Nonlinear Sci. 22 (2012), 371–398.
[3] A. Ali, H. Kalisch. *On the formulation of mass, momentum and energy conservation in the KdV equation.* Acta Appl. Math. 133 (2014), 113–131.
[4] T.B. Benjamin, M.J. Lighthill. *On cnoidal waves and bores.* Proc. Roy. Soc. London A 224 (1954), 448–460.
[5] J.L. Bona, M. Chen, J.-C. Saut. *Boussinesq equations and other systems for small-amplitude long waves in nonlinear dispersive media. I: Derivation and linear theory.* J. Nonlinear Sci. 12 (2002), 283–318.
[6] J.L. Bona, M. Chen, J.-C. Saut. *Boussinesq equations and other systems for small-amplitude long waves in nonlinear dispersive media. II: The nonlinear theory.* Nonlinearity 17 (2004), 925–952.
[7] J.L. Bona, T. Colin, D. Lannes. *Long wave approximations for water waves.* Arch. Ration. Mech. Anal. 178 (2005), 373–410.
[8] J. Boussinesq. *Théorie des ondes et des remous qui se propagent le long d'un canal rectangulaire horizontal, en communiquant au liquide contenu dans ce canal des vitesses sensiblement pareilles de la surface au fond.* J. Math. Pures Appl. 17 (1872), 55–108.
[9] C.I. Christov. *An energy-consistent dispersive shallow-water model.* Wave Motion 34 (2001), 161–174.
[10] W. Craig , M.D. Groves. *Hamiltonian long-wave approximations to the water-wave problem.* Wave Motion, 19 (1994), 367–389.
[11] W. Craig, P. Guyenne, H. Kalisch. *A new model for large amplitude long internal waves.* Comptes Rendus Mecanique 332 (2004), 525–530.
[12] W. Craig, P. Guyenne, H. Kalisch. *Hamiltonian long-wave expansions for free surfaces and interfaces.* Comm. Pure Appl. Math. 58 (2005), 1587–1641.
[13] W. Craig, C. Sulem. *Numerical simulation of gravity waves.* J. Comp. Phys. 108 (1993), 73–83.
[14] D. Dutykh, F. Dias. *Energy of tsunami waves generated by bottom motion.* Proc. R. Soc. Lond. Ser. A 465 (2009), 725–744.
[15] S. Gavrilyuk, H. Kalisch, Z. Khorsand. *A kinematic conservation law in free surface flow.* Nonlinearity 28 (2015), 1805–1821.
[16] H. Kalisch, Z. Khorsand, D. Mitsotakis. *Mechanical balance laws for fully nonlinear and weakly dispersive water waves.* Physica D 333 (2016), 243–253.
[17] H. Kalisch and A. Senthilkumar. *Derivation of Boussinesq's shoaling law using a coupled BBM system.* Nonlin. Processes Geophys. 20 (2013), 213–219.
[18] D.J. Kaup. *A higher-order wave equation and the method for solving it.* Prog. Theor. Phys. 54 (1975), 396–408.
[19] Z. Khorsand, H. Kalisch. *On the shoaling of solitary waves in the KdV equation.* Proc. 34th Conf. Coastal Engineering, Seoul, Korea, 2014, Vol. 34, 10 pp.
[20] D. Lannes. The water wave problem. Mathematical Surveys and Monographs, vol. 188. Amer. Math. Soc., Providence, 2013.
[21] D. Lannes, P. Bonneton. *Derivation of asymptotic two-dimensional time-dependent equations for surface water wave propagation.* Phys. Fluids 21 (2009), 016601.
[22] D. Moldabayev, H. Kalisch, D. Dutykh *The Whitham Equation as a model for surface water waves* Physica D 309 (2015), 99–107.
[23] D.P. Nicholls, F. Reitich. *A new approach to analyticity of Dirichlet-Neumann operators.* Proc. Roy. Soc. Edinburgh Sect. A 131 (2001), 1411–1433.
[24] O. Nwogu. *Alternative form of Boussinesq equations for nearshore wave propagation.* J. Waterway, Port, Coastal and Ocean Engineering 119 (1993), 618–638.
[25] D.H. Peregrine. *Long waves on a beach.* J. Fluid Mech. 27 (1967), 815–827.
[26] A.A. Petrov. *Variational statement of the problem of liquid motion in a container of finite dimensions.* Prikl. Math. Mekh. 28 (1964), 917–922.
[27] D.H. Peregrine, *Equations for water waves and the approximation behind them.* in 'Waves on beaches and resulting sediment transport'; proceedings of an advanced seminar conducted by the Mathematics Research Center, (New York, Academic Press, 1972, pp. 95–121).
[28] J.J. Stoker. Water waves: the mathematical theory with applications. Pure and Applied Mathematics, Vol. IV. Interscience Publishers, New York, 1957.
[29] I.A. Svendsen, O. Brink-Kjær. *Shoaling of cnoidal waves.* Proc. 13th Conf. Coastal Engng, Vancouver, 1972, pp. 365–383.
[30] I.A. Svendsen, J. Buhr Hansen. *The wave height variation for regular waves in shoaling water.* Coastal Engineering 1 (1977), 261–284.
[31] G.B. Whitham. Linear and nonlinear waves. Wiley, New York, 1974.
[32] V.E. Zakharov, *Stability of periodic waves of finite amplitude on the surface of a deep fluid.* J. Appl. Mech. Tech. Phys. 9 (1968), 190–194.